

Calculations of DOS and electronic structure in Bi_2S_3 and Bi_2Se_3 by using FP-LAPW method

Dandeswar Deka¹, A. Rahman¹ and R. K. Thapa

Department of Physics, Condensed Matter Theory Research Group, Mizoram University, Aizawl 796 004, Mizoram

¹Department of Physics, Gauhati University, Guwahati 781014

Email: d.deka2010@rediffmail.com

Abstract

The electronic structures for Bi_2S_3 and Bi_2Se_3 have been investigated by first principles full potential-linearized augmented plane wave (FP-LAPW) method with Generalized Gradient Approximation (GGA). The calculated density of states (DOS) and band structures show semiconducting behavior of Bi_2S_3 and Bi_2Se_3 with a narrow indirect energy band gap of 1.4 eV in Bi_2S_3 and 0.8 eV in Bi_2Se_3 .

Keywords: DFT, FP-LAPW, DOS, energy band structure, energy band gap.

PACS: 71.15.-m, 71.15.Dx, 71.15.Mb, 71.20.-b, 75.10.-b

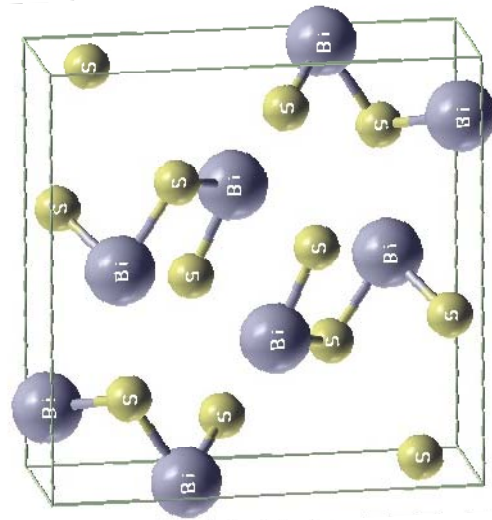
1. INTRODUCTION

Today semiconductors can be grown with various compositions from monoatomic layer to nano-scale islands, rows, arrays, in the art of quantum technologies and the numbers of conceivable new electronic devices are manufactured [1]. Narrow gap semiconductors Bi_2S_3 and Bi_2Se_3 are classic room temperature thermoelectric materials[2]. These are the chalcogenides of poor metal having important technological applications in optoelectronic nano devices [3], field-emission electronic devices [4], photo-detectors and photo-electronic devices [5] and photovoltaic converters, thermoelectric cooling technologies based on the Peltier effect [6,7]. They have orthorhombic crystal structures at room temperature with x, y and z- positions of atoms [8] as given in Table:1 and space group Pnma (number 62). The crystal structures of Bi_2S_3 and Bi_2Se_3 are illustrated in Fig.1(a-b). In this report, we would like to present a systematic study of DOS and energy band structures of Bi_2S_3 and Bi_2Se_3 using FP-LAPW method.

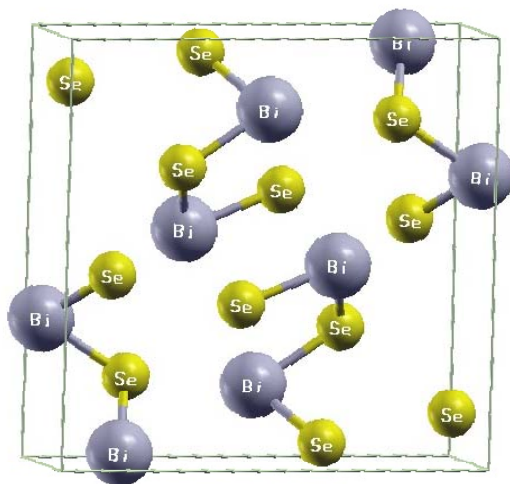
Se 2	0.870	0.25	0.556
Se 3	0.213	0.25	0.193

Table 1: x, y and z-positions of atoms of Bi_2S_3 and Bi_2Se_3

Atom (Bi_2S_3)	X	Y	Z
Bi 1	0.0164	0.25	0.6745
Bi 2	0.3406	0.25	0.4661
S 1	0.0494	0.25	0.1311
S 2	0.3773	0.25	0.0604
S 3	0.2165	0.25	0.8069
Atom (Bi_2Se_3)	X	Y	Z
Bi 1	0.012	0.25	0.328
Bi 2	0.343	0.25	0.534
Se 1	0.067	0.25	0.876



(a) Bi_2S_3



(b) Bi₂Se₃

Fig.1 : Unit cell structures of Bi₂S₃ and Bi₂Se₃

2. THEORY AND COMPUTATIONAL METHODS

First principles FP-LAPW [9] method based on density functional theory (DFT) is used for calculations of DOS and band structure of Bi₂S₃. The version of GGA as prescribed by Perdew, Burke and Ernzerhof [10] was used for the exchange and correlation potentials. The calculated total energy (E) within GGA as a function of the volume (V) were used for determination of theoretical lattice constants. Equilibrium lattice constants are calculated by fitting the calculated total energy to the Murnaghan’s equation of state [11]. A series of total energy calculations as a function of volume can be fitted to an equation of states according to Murnaghan.

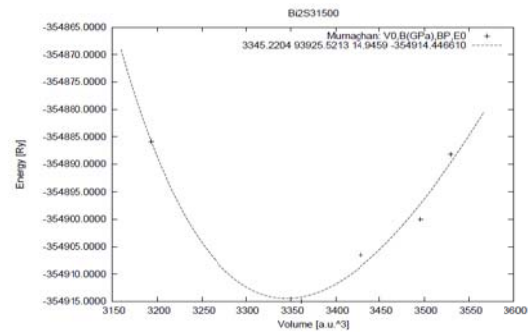
$$E(V) = E_0 + \frac{\left(\frac{V_0}{V}\right)^{B_0} B_0}{B_0 - 1} + \frac{B_0 V_0}{B_0 - 1} \quad (1)$$

where E_0 is the minimum energy at $T = 0K$, B_0 is the bulk modulus at the equilibrium volume and B_0' is pressure derivative of the bulk modulus at the equilibrium volume. The equilibrium volume is given by the corresponding total energy minimum as shown in Fig.2(a-b) [12]. The equilibrium lattice constant was optimized using the experimental values of $a=11.269 \text{ \AA}$, $b=3.9717 \text{ \AA}$ and $c= 11.129 \text{ \AA}$ for Bi₂S₃, and $a= 11.83 \text{ \AA}$, $b=4.09 \text{ \AA}$ and $c=11.62 \text{ \AA}$ for Bi₂Se₃ [8]. The calculation was accomplished by using the WIEN2K code [13]. In the FP-LAPW procedure , wave functions, charge density and potential are expanded in spherical harmonics within non overlapping atomic spheres of radius R_{mt} and in the remaining space of the unit cell plane waves are considered. The maximum multi-polarity l for the waves inside the atomic spheres was confined within $l_{max}= 10$. The wave functions in the interstitial region were expanded in plane waves with a cut-off of to $K_{max}=2.5 \text{ a.u.}^{-1}$ (where K_{max} is the maximum value of the wave vector $\mathbf{K}=\mathbf{k}+\mathbf{G}$). For Bi: $6s, 6p$, S: $3s, 3p$ and Se: $4s, 4p$ states were treated as valance state and all other lower states were treated as core state. The potential and charge density were expanded upto a cut-off $G_{max} = 12 \text{ a.u.}^{-1}$. The muffin- tin radii are set to $R_{mt} = 2.4 \text{ a.u.}$ for Bi and 2.2 a.u. for S in Bi₂S₃ and $R_{mt} = 2.3 \text{ a.u.}$ for Bi and 2.2 a.u. for Se in Bi₂Se₃. A mesh of 1500 k-points was used after doing k- optimization. The calculated lattice constants found by volume optimization are $a= 11.2263 \text{ \AA}$, $b= 3.567 \text{ \AA}$ and $c= 11.0868 \text{ \AA}$ for Bi₂S₃, and $a=11.4753 \text{ \AA}$, $b= 3.9647 \text{ \AA}$ and $c= 11.2716 \text{ \AA}$ for Bi₂Se₃ which are shown in Fig.2(a-b).

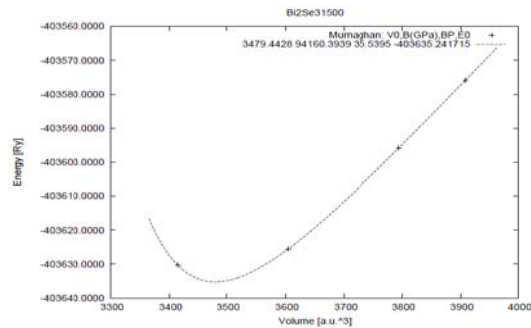
Table 2: The parameters chosen for the computation of Bi₂S₃ and Bi₂Se₃

PARAMETERS	VALUES USED
The plane-wave cut-off for the basis functions , $R_{MT} \times K_{max}$	7
Expansion of wave functions,density, potentials inside the R_{MT} , l_{max}	10
The potential, charge density	12 a.u.^{-1} .

expanded upto cut-off , G_{max}	
Number of plane waves generated	729
Wave vector, k	1500
R_{MT} used	Bi = 2.4 a.u., S = 2.2 a.u. (for Bi ₂ S ₃) Bi = 2.3 a.u.,Se= 2.2 a.u. (for Bi ₂ Se ₃)



(a) Bi₂S₃



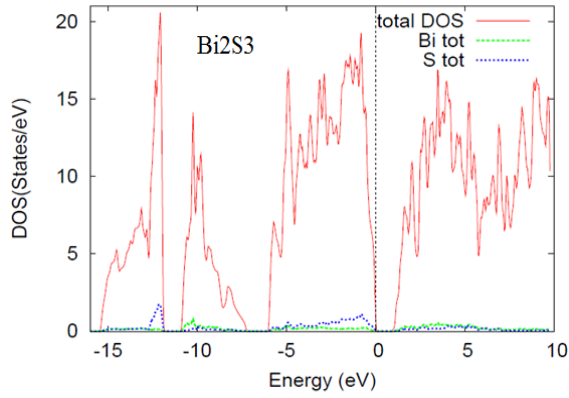
(b) Bi₂Se₃

Fig. 2: Energy versus Volume curve using the volume optimization method for Bi₂S₃and Bi₂Se₃

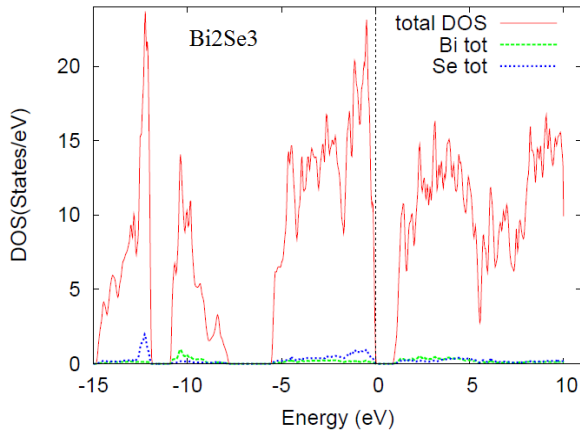
3. RESULTS AND DISCUSSIONS

In Fig.2(a-b), we show the total energy curve as a function of unit cell volume for Bi₂S₃ and Bi₂Se₃. The total and partial DOS plots of Bi₂S₃ and Bi₂Se₃ are shown in Figs.3,4,5 & 6. From Fig.3, we found that the contributions to total DOS were from Bi- $6p$ and S- $3p$ electron states in Bi₂S₃ and from Bi- $6p$ and Se- $4p$ electron states in Bi₂Se₃. The core region which is below -6eV is formed by $6s$ and $6p$ electron states of Bi and a sharp peak at around -10.5 eV is observed in Bi₂S₃[Fig.4(a)] and a sharp peak at around -10.2 eV is observed in Bi₂Se₃[Fig.4(b)]. The conduction region, which is above the Fermi level, is mainly contributed by Bi- $6p$, $6p_x$, $6p_y$ state electrons in Bi₂S₃[Fig.5(a)]

and by Bi- $6p$, $6p_x$ state electrons in Bi_2Se_3 [Fig.5(b)]. In the valence region (below Fermi level), we have observed, S- $3p$ electron state is mainly contributing to total DOS giving a sharp peak at around -0.8eV in Bi_2S_3 [Fig.6(a)] and Se- $4p$ electron state is mainly contributing to total DOS giving sharp peaks at around -0.5eV and -1.2eV in Bi_2Se_3 [Fig.6(b)].

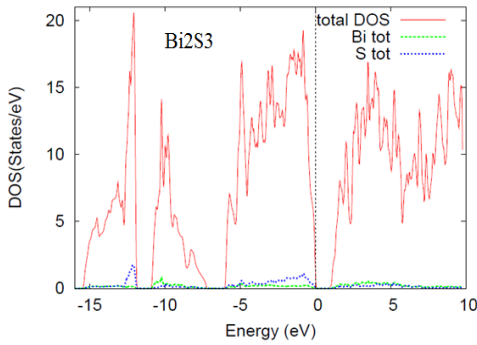


(a) Bi_2S_3

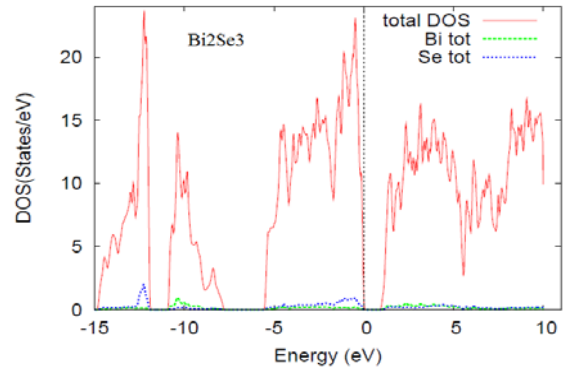


(b) Bi_2Se_3

Fig. 3: Bi_2S_3 -total, Bi-total and S-total and Bi_2Se_3 -total, Bi-total and Se-total (Energy= 0 eV, corresponds to Fermi level)

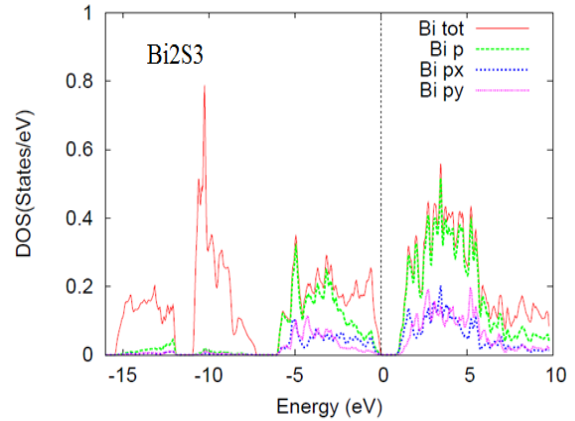


(a) Bi_2S_3

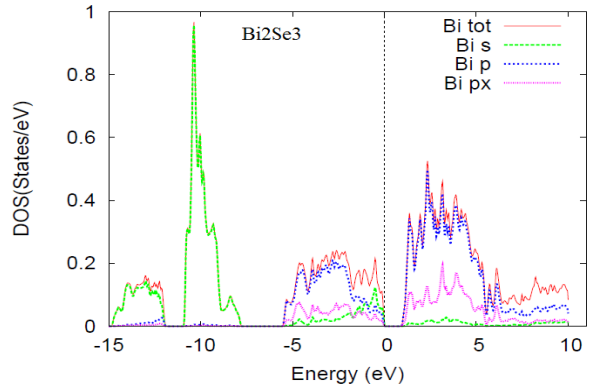


(b) Bi_2Se_3

Fig. 4 : Total DOS, Bi-total & S-total states of Bi_2S_3 and Total DOS, Bi-total & Se-total states of Bi_2Se_3



(a) Bi_2S_3



(b) Bi_2Se_3

Fig.5: Bi-total, Bi- p , p_x & p_y states of Bi_2S_3 and Bi-total, Bi- s , p & p_x states of Bi_2Se_3

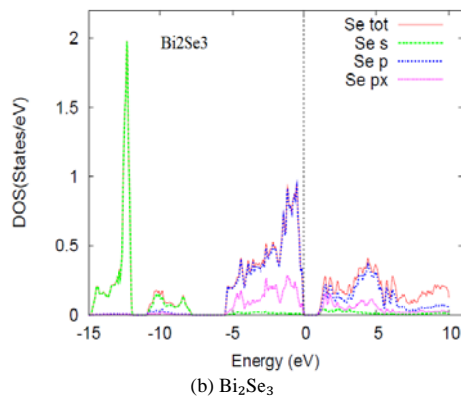
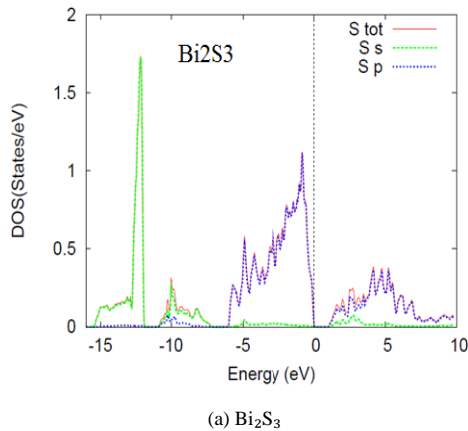


Fig.6: S-total, S-s & S-p States of Bi_2S_3 and Se-total, Se-s, Se-p & Se- p_x States of Bi_2Se_3

From the band structure plots, we observed an indirect band gap of the order of 1.4 eV in Bi_2S_3 [Fig.7(a)]and an indirect band gap of the order of 0.8 eV in Bi_2Se_3 [Fig.7(b)]. The band structure plots were also found with higher number of bands at the regions where peaks of the DOS were observed. In Fig.8 & 9 we have compared band structures with DOS plots of Bi_2S_3 and Bi_2Se_3 , and found that higher DOS regions correspond to more bands.

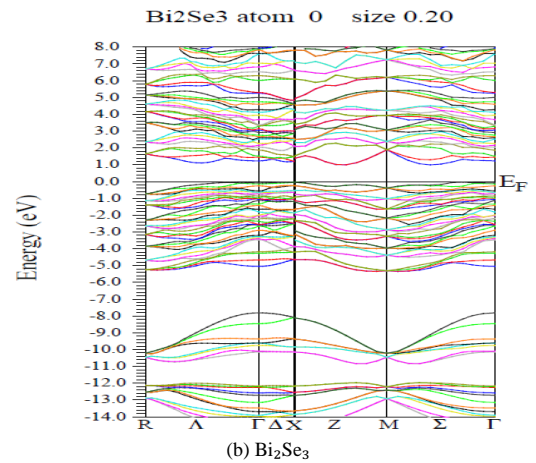
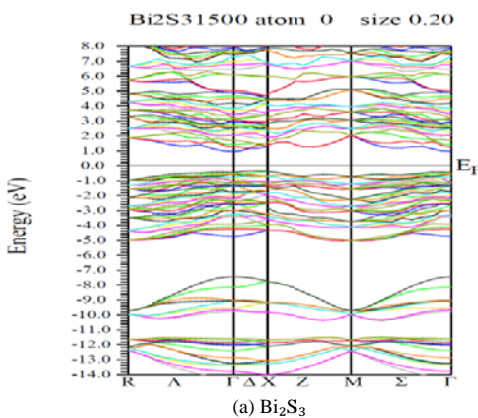
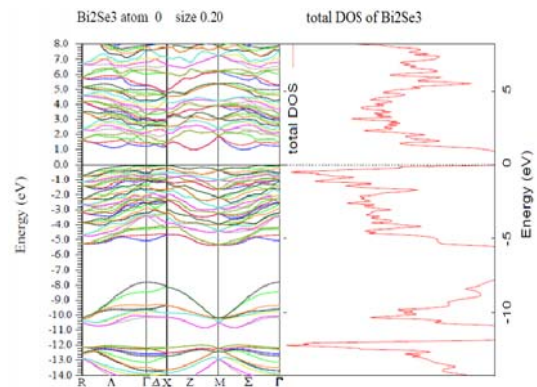
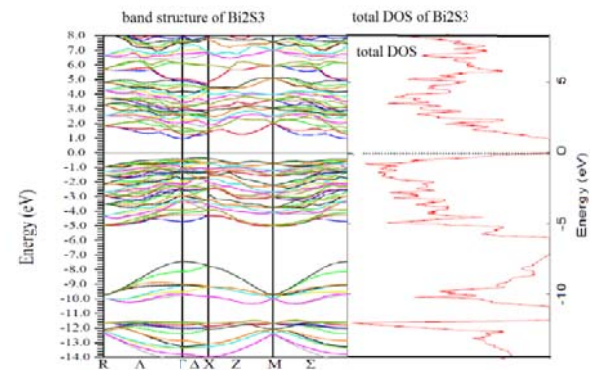


Fig.7: The plots of band structures of Bi_2S_3 and Bi_2Se_3



4. CONCLUSIONS

In conclusion, we have observed a qualitative agreement between theoretical and experimental lattice constants. Calculated band

gap is very close to experimental value. Band gaps of the order of 1.4 eV and 0.8eV suggest that Bi_2S_3 and Bi_2Se_3 are semiconductors with low energy gap. Since Fermi level is very close to valance band, it indicates that the semiconductors are p-type. The calculated band gaps also suggest that the compounds may be used as suitable candidate for thermoelectric applications. The semiconductor Bi_2S_3 with band gap 1.4eV belongs to a family of solid state materials with applications in thermoelectric cooling technologies based on the Peltier effect [14,15]. The semiconductor Bi_2Se_3 with band gap 0.8eV has useful applications in the field of thermoelectric devices as solid state coolers or generators [16,17]. However, the band gaps when checked with experimental values (1.3eV in Bi_2S_3 and 0.8eV in Bi_2Se_3) [14] seem to have differences. We propose to check these discrepancies with mBJ potential inclusion.

ACKNOWLEDGEMENTS

DD is grateful to Department of Physics, Gauhati University and Department of Physics, Mizoram University for extending all the necessary facilities for doing this work. RKT acknowledges a research grant from UGC.

REFERENCES

- [1] E. Erbarut, Solid State Communications, **127**, 515-519 (2003).
- [2] M.G. Kanatzidis, Semiconductors and Semimetals, **69**, 51 (2001).
- [3] H. Bao, X. Cui, C. Li, Y. Gan, J. Zhang and J. Guo Photoswitchable Semiconductor Bismuth Sulfide (Bi_2S_3) Nanowires and Their Self-Supported Nanowire Arrays, *J. Phys. Chem. C*, **111**(33), 12279-12283 (2007).
- [4] Y. Yu, C. H. Jin, R. H. Wang, Q. Chen and L. M. Peng, High Quality Ultralong Bi_2S_3 Nanowires : Structure, Growth and Properties, *J. Phys. Chem. B*, **109**(40), 18772-18776 (2005).
- [5] L. Li, R. Cao, Z. Wang, J. Li and L. Qi, Template Synthesis of Hierarchical Bi_2E_3 (E= S, Se, Te) Core-Shell microspheres and Their Electrochemical and Photoresponsive Properties, *J. Phys. Chem. C*, **113**(42), 18075-18081 (2009).
- [6] B. Miller, A. Heller, Semiconductor liquid junction solar cells based on anodic sulphide films, *Nature* **262**, 680-681 (1976).
- [7] O. Rabin, J.M. Perez, J. Grimm, G. Wojtkiewicz, R. Weissleder, An X-ray computed tomography imaging agent based on long-circulating bismuth sulphide nanoparticles, *Nat. Mater.* **5**, 118 (2006).
- [8] L. F. Lundegaard, E. Makovicky, T. Boffa Ballaran and T. Balic-Zunic, Crystal structure and cation lone electron pair activity of Bi_2S_3 between 0 and 10 GPa *Physics and Chemistry of Minerals* **32**, 578-584 (2005).
- [9] R. K.Thapa, Sandeep, M. P. Ghimire and Lalmuanpuia, Study of DOS and energy band structures in beryllium chalcogenides, *Indian J. Phys.* **85**, 727-736 (2011).
- [10] J. P. Perdew, K. Burke and M. Ernzerhof, Generalized Gradient Approximation Made Simple, *Phys. Rev. Lett.*, **77**, 3865 (1996).
- [11] F. D. Murnaghan, The compressibility of media under extreme pressures, *Proc. Natl. Acad. Sci. USA* **30**, 244-247 (1944).
- [12] P. Schwartz and P. Blaha, Fifth World Congress on Computational Mechanics, Vienna, Austria (1903).
- [13] P. Blaha, K. Schwarz, G. Madsen, D. Kvasnicka and J. Luitz, An Augmented Plane Wave Plus Local Orbitals Program for calculating Crystal Properties (Tech. University, Vienna-Austria) (2001).
- [14] J. Black, E. M. Conwell, L. Seigle and C. W. Spencer, Electrical and optical properties of some $\text{M}_2^{\text{V-B}}\text{N}_3^{\text{VI-B}}$ semiconductors, *J. Physics and Chemistry of Solids* **2**(3), 240-251, (1957).
- [15] X. S. Peng, G. W. Meng, J. Zhang, L. X. Zhao, X. F. Wang, Y. W. Wang, L. P. Zhang, Electrochemical fabrication of ordered Bi_2S_3 nanowire arrays, *J. Phy. D: Appl. Phys.* **34**, 3224(2001).
- [16] D. M. Rowe, CRC Hand book of Thermoelectrics, CRC press, Boca Ratou, FL, 90 (1995).
- [17] H. J. Goldsmith, Thermoelectric Refrigeration, Pion Ltd., London (1986).